

reverse transcriptase (RT) was used for first strand synthesis; second strand synthesis was with the Klenow fragment of DNA polymerase I followed by M-MuLV RT. cDNAs were treated with S1 nuclease, methylated, size-fractionated on Sepharose 4B, ligated to  $\lambda$ gt11 arms, and packaged. The library consists of  $25 \times 10^6$  independent recombinants with inserts  $>500$  bp.

20. A. M. Maxam and W. Gilbert, *Proc. Natl. Acad. Sci. U.S.A.* **74**, 560 (1977).
21. R. V. Lebo *et al.*, *Science* **225**, 57 (1984).
22. P. A. Krieg and D. A. Melton, *Nucleic Acids Res.* **12**, 7057 (1984); S. M. Hollenberg *et al.*, *Nature (London)* **318**, 635 (1985).
23. For in vitro transcription, the entire Eco RI insert of rbeA12 was cloned into pGEM1 (Promega Biotec). A second construction deleting 227 bp of 5' untranslated sequence, rbeA12B, was made by inserting the T<sub>4</sub> DNA polymerase-filled Bgl I-Sma I fragment of rbeA12 (nucleotide position 227 to the polylinker) into the Sma I site of pGEM3. For thyroid hormone binding, transcriptions were performed with SP6 polymerase and 5 to 10  $\mu$ g of rbeA12B linearized with Sst I. Transcripts were purified by P60 chromatography and translated in 150 to 200  $\mu$ l of rabbit reticulocyte lysate (Promega Biotec) in conditions suggested by the manufacturer. Thyroid hormone binding for both the Scatchard and competi-
24. J. M. Chirgwin, A. F. Przybyla, R. J. MacDonald, W. F. Rutter, *Biochemistry* **18**, 5294 (1979).
25. M. M. Harpold, R. M. Evans, M. Salditt-Georgieff, J. E. Darnell, *Cell* **17**, 1025 (1979).
26. We thank I. Akerblom, S. Hollenberg, and especially J. Arriza for helpful suggestions, G. Cerelli for invaluable sequencing consultations, and B. Sefton and D. Gruol for critically reading the manuscript. C.C.T. is supported by a predoctoral training grant to the Department of Biology, University of California, San Diego. C.W. and R.L. are research associates and R.M.E. an investigator of the Howard Hughes Medical Institute. Supported by grants from the NIH (GM-266444-09) and the Howard Hughes Medical Institute.

## Evidence for Dispensable Sequences Inserted into a Nucleotide Fold

RUTH M. STARZYK, TERESA A. WEBSTER, PAUL SCHIMMEL

Previous experimental results along with the structural modeling presented indicate that a nucleotide fold starts in the amino-terminal part of *Escherichia coli* isoleucyl-transfer RNA synthetase, a single chain polypeptide of 939 amino acids. Internal deletions were created in the region of the nucleotide fold. A set of deletions that collectively span 145 contiguous amino acids yielded active enzymes. Further extensions of the deletions yielded inactive or unstable proteins. The three-dimensional structure of an evidently homologous protein suggests that the active deletions lack portions of a segment that connects two parts of the nucleotide fold. Therefore, the results imply that removal of major sections of the polypeptide that connects these two parts of the fold does not result in major perturbation of the nucleotide binding site.

IT IS POSSIBLE TO DISSECT PROTEINS into pieces and to investigate activities and structures of fragments (1-3). The delineation of substructures within a structure provides a starting point for making chimeric enzymes, in which components of two or more enzymes are recombined to give a new species. There is evidence that such recombination occurs in nature (4, 5).

Aminoacyl-transfer RNA synthetases are a class of proteins that catalyze aminoacylation of specific transfer RNAs in a two-step reaction: condensation of adenosine triphosphate (ATP) with amino acid to give an enzyme-bound aminoacyl adenylate, and reaction of the bound adenylate with transfer RNA (tRNA) to give aminoacyl-tRNA (6). Although these enzymes catalyze the same reaction for each amino acid, there is considerable variability in the gross structural features of the proteins (for example, different quaternary structures or subunit sizes).

Structural analysis has shown that a domain resembling a nucleotide binding fold (Rossmann fold) (7) occurs in the NH<sub>2</sub>-terminal part of the *Escherichia coli* methionine (8-10) and *Bacillus stearothermophilus* tyrosyl-tRNA synthetases (11, 12). There is further evidence that a similar fold occurs in the NH<sub>2</sub>-terminal parts of several other aminoacyl-tRNA synthetases (6).

Apart from the delineation of dispensable sequences in the COOH-terminal halves of two aminoacyl-tRNA synthetases (1, 13, 14), there is no evidence for insertions of expendable sequences that interrupt a structural or functional domain within these enzymes. We now present evidence that a large, dispensable sequence is inserted into the nucleotide fold of a large aminoacyl-tRNA synthetase.

The  $\alpha$ - $\beta$  structure that forms the nucleotide binding fold of *E. coli* methionyl-tRNA synthetase (8-10) (Fig. 1) is made up of

approximately the first 360 residues of the 677 amino acid subunit (10, 15, 16). We adopted the nomenclature for lactate dehydrogenase and assigned letter designations to the individual elements of  $\beta$  structure and  $\alpha$  helix (7). In this prototypical representation of the Rossmann nucleotide fold, there are six strands of parallel sheet with two  $\alpha$  helices on either side of the  $\beta$  structure (7). The secondary structural element boundaries indicated in Fig. 1 are in accordance with the most recent structural analyses by Brunie and co-workers (10).

The nucleotide fold is divided more or less into two halves, each of which comprises three  $\beta$  strands and two  $\alpha$  helices. The first half is made up of approximately the NH<sub>2</sub>-terminal 97 amino acids and the second half starts around amino acid residue 226 and continues to about amino acid residue 361. The two halves are separated by a segment of roughly 127 amino acids which starts at the COOH-terminal end of  $\beta_C$ . We designate this segment connective polypeptide one (CP1). While this segment contains elements of defined secondary structure, which includes a helix that lies parallel to the  $\beta$  sheet, it is not part of the prototypical nucleotide fold of Fig. 1. The second half of the methionine synthetase nucleotide fold is further interrupted by a segment (designated CP2) of about 70 amino acids, which starts at the COOH-terminal end of  $\beta_D$ .

In contrast to the dimeric methionyl-tRNA synthetase (6), isoleucyl-tRNA synthetase is a monomer of 939 amino acids (6, 17). While there is no three-dimensional structural information on this enzyme, amino acids 58 to 68 have ten identities and one conservative substitution when aligned with amino acids 14 to 24 of the methionine enzyme (17) (Fig. 1). The match includes the connecting segment between the COOH-terminal end of  $\beta_A$  and the NH<sub>2</sub>-terminal end of  $\alpha_B$  and extends somewhat into the latter structure.

This element is a signature sequence for a subclass of aminoacyl-tRNA synthetases and is likely to correspond to the same three-dimensional structural component in these enzymes (17, 18). In the case of the *B. stearothermophilus* tyrosine enzyme, close structural homology with the *E. coli* methionyl-tRNA synthetase in this general region has been demonstrated. This homology of structure extends over  $\beta_A$ ,  $\alpha_B$ , and  $\beta_B$ , even though the two enzymes have no significant sequence match beyond that of the signature

R. M. Starzyk and P. Schimmel, Department of Biology, Massachusetts Institute of Technology, Cambridge, MA 02139.

T. A. Webster, Molecular Biology Computer Research Resource, Dana-Farber Cancer Institute, Harvard School of Public Health, Boston, MA 02115.

sequence. In the methionine enzyme, Gly<sup>23</sup> (in the signature sequence) structurally corresponds to the last glycine (19) of the GXXGXG sequence at the corner between  $\beta_A$  and  $\alpha_B$  of the Rossmann fold (7-9, 20).

A second region of sequence similarity between the methionine and isoleucine enzymes occurs at positions 329 to 338 and 599 to 608, respectively (21-23). This contains seven identities and one conservative change out of ten residues. This stretch includes a lysine that is labeled by the 3'-adenosine dialdehyde derivative of tRNA<sup>fMet</sup> (21). It forms part of the connecting loop between  $\beta_E$  and  $\alpha_F$  (Fig. 1).

We attempted to model the unknown isoleucyl-tRNA synthetase structure with the known nucleotide fold of the methionine enzyme. The enzyme polypeptides differ by 262 amino acids, and it occurred to us that some of this length variation might occur in CP1 and CP2. We found an interrupted alignment of sequences across 151 amino acids of methionyl-tRNA synthetase that begins just before the signature sequence and ends just after the aforementioned sequence similarity at positions 329 to 338 (Fig. 2). The identical or similar amino acids are boxed and extend from position 4 to 358 of the methionine enzyme to give a 53% similarity between the two sequences. This alignment, however, is interrupted at two places. In the methionine sequence, one interruption occurs between positions 89 and 208 and spans  $\beta_C$  and almost all of CP1 (Fig. 1). The length of this gap in the alignment is 118 and 316 amino acids, respectively, for the methionine and isoleucine enzymes. The occurrence of large, nonhomologous segments of markedly unequal sizes could explain why more extensive sequence relations between synthetases have not previously been identified by us or others.

The second gap starts at the COOH-terminal end of  $\beta_D$  and continues through CP2 and  $\alpha_E$  to the NH<sub>2</sub>-terminal end of  $\beta_E$ . This gap corresponds to 87 and 115 amino acids, respectively, in the methionine and isoleucine enzymes.

Only  $\beta_C$  and  $\alpha_E$  with its connecting loop, in addition to CP1 and CP2, show no discernible amino acid sequence homology (Fig. 1). Much of the large length difference between the two enzymes can be attributed to the segment designated CP1. To test further the structural relationship between the two synthetases, and the significance of CP1, we created seven internal deletions within *ileS* (Fig. 3). These deletions collectively span the region between codons 177 and 499 so that each starts after  $\alpha_C$  of methionyl-tRNA synthetase and collectively encompass the entire region designated as

CP1 and somewhat beyond. The individual deletions range in size from 44 to 321 amino acids.

Maxicell synthesis of the deletion proteins (24) gives an enhanced visualization of plasmid-encoded polypeptides (Fig. 4). With the exception of the two largest internal

deletions, each deletion protein is synthesized in amounts comparable to wild-type Ile-tRNA synthetase. The sizes of each protein correspond to the expected size based on the particular deletion that was created. This suggests that most of the truncated proteins are, at least in maxicells, relatively

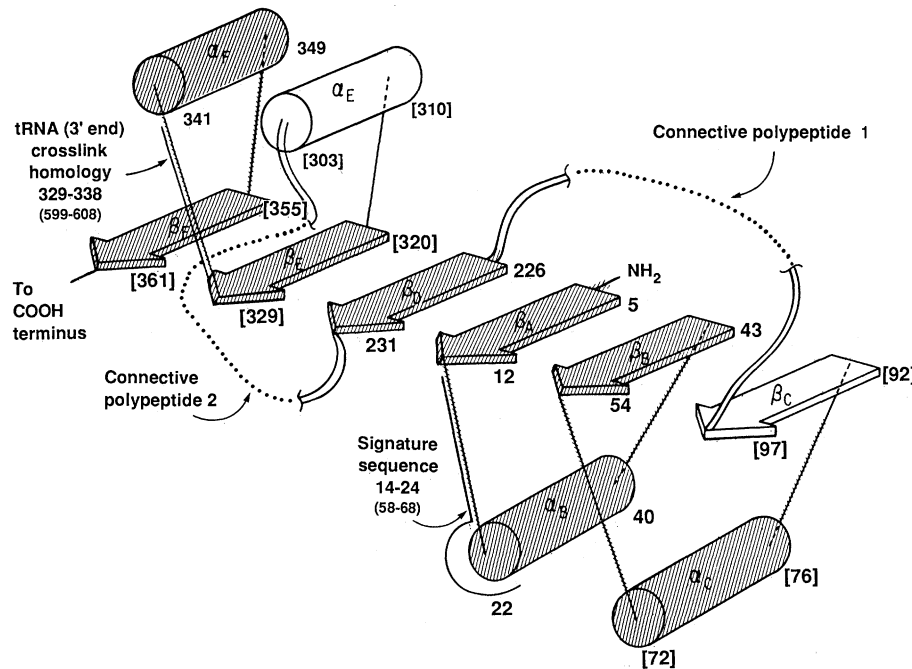


**Fig. 1.** Schematic representation of the *E. coli* Met-tRNA synthetase nucleotide fold. Boundaries for the  $\alpha$  helices (cylinders) and  $\beta$  strands (arrows) are indicated with preliminary assignments of amino acids in brackets. Corresponding amino acids in Ile-tRNA synthetase are numbered in parenthesis. Regions of amino acid sequence similarity from Fig. 2 are shown by shading. [This figure is a modified version of Fig. 7b of (9).]

**Fig. 2.** Comparative sequence analysis of *E. coli* Met- and Ile-tRNA synthetases. The standard dynamic programming sequence comparison method (30) was executed by LOCAL (31) to generate local optimal alignments and their corresponding similarity scores between Met- and Ile-tRNA synthetase. Similarity scores for the matches involving residues 1 to 100 ( $\beta_A$ - $\beta_C$ ) and 302 to 360 ( $\alpha_E$ - $\beta_F$ ) of Met-tRNA synthetase are potentially significant ( $z = 7.7$  and  $3.9$ , respectively) (32). Functional significance for Ile-tRNA synthetase residues 450 to 472 is suggested by the match to Val-tRNA synthetase from *E. coli*, *B. stearothermophilus* (33), and yeast (34), and the inclusion of Cys<sup>463</sup> in the alignment (circled). [Cys<sup>463</sup> is affinity-labeled by an isoleucine analog (35, 36)]. The conservative limited amino acid alphabet used is (single letter abbreviation) (19): A=G, D=E, N=Q, I=L=V, F=W=Y, H=K=R, S=T, C, M, P. The Lys<sup>335</sup> of Met-tRNA synthetase, which is labeled by the 3'-adenosine dialdehyde derivative of tRNA<sup>fMet</sup> (21), is circled.

MetRS	... <sup>4</sup> AKK-I <sup>1</sup> LVTCA <sup>1</sup> LPYANGSIHLGHML <sup>1</sup> EHI <sup>1</sup> QA <sup>31</sup>
IleRS	... <sup>47</sup> GKKTF <sup>1</sup> ILHDGP <sup>1</sup> PPYANGSIHIGHS <sup>1</sup> VN <sup>1</sup> KIL <sup>1</sup> KL <sup>75</sup>
MetRS	<sup>32</sup> D <sup>1</sup> VWR <sup>1</sup> YQRM <sup>1</sup> R <sup>1</sup> GHE <sup>1</sup> VNF <sup>1</sup> ICADD <sup>1</sup> AHGT <sup>1</sup> PI <sup>1</sup> ML <sup>1</sup> K <sup>61</sup>
IleRS	<sup>76</sup> D <sup>1</sup> IIV <sup>1</sup> KS <sup>1</sup> GL <sup>1</sup> SGY <sup>1</sup> DSPY <sup>1</sup> VPG <sup>1</sup> WD <sup>1</sup> CHGL <sup>1</sup> PI <sup>1</sup> EL <sup>1</sup> K <sup>105</sup>
MetRS	<sup>62</sup> A <sup>1</sup> QQLGIT <sup>1</sup> P-E <sup>1</sup> QMI <sup>1</sup> GE <sup>1</sup> MSQE <sup>1</sup> H <sup>1</sup> Q <sup>1</sup> TDFAG <sup>1</sup> FN <sup>1</sup> I <sup>89</sup>
IleRS	<sup>106</sup> V <sup>1</sup> EQEY <sup>1</sup> GK <sup>1</sup> PG <sup>1</sup> E <sup>1</sup> KFT <sup>1</sup> AAEF <sup>1</sup> RA <sup>1</sup> K <sup>1</sup> CRE <sup>1</sup> YAAT <sup>1</sup> QV <sup>1</sup> I <sup>134</sup>
MetRS	<sup>298</sup> G <sup>1</sup> AL <sup>1</sup> QE <sup>1</sup> QVANK <sup>1</sup> M <sup>1</sup> Q <sup>1</sup> WFES <sup>1</sup> GL <sup>1</sup> Q <sup>1</sup> Q <sup>1</sup> WD <sup>1</sup> I <sup>231</sup>
IleRS	<sup>450</sup> AR <sup>1</sup> IES <sup>1</sup> MVAN <sup>1</sup> R-PD <sup>1</sup> WC <sup>1</sup> IS <sup>1</sup> R <sup>1</sup> Q <sup>1</sup> RT <sup>1</sup> WG <sup>1</sup> V <sup>472</sup>
	ValRS <sup>421</sup> D <sup>1</sup> WCIS <sup>1</sup> R <sup>1</sup> QL <sup>1</sup> WW <sup>1</sup> GH <sup>432</sup>
MetRS	<sup>319</sup> N <sup>1</sup> LVHGY <sup>1</sup> -V <sup>1</sup> T <sup>1</sup> VNGAK <sup>1</sup> MS <sup>1</sup> (K <sup>1</sup> )SR <sup>1</sup> G <sup>1</sup> T <sup>339</sup>
IleRS	<sup>588</sup> Q <sup>1</sup> VLTHGF <sup>1</sup> TV <sup>1</sup> D <sup>1</sup> GGR <sup>1</sup> KMS <sup>1</sup> KS <sup>1</sup> I <sup>1</sup> GN <sup>609</sup>
MetRS	<sup>340</sup> F <sup>1</sup> IKASTWL <sup>1</sup> NHF <sup>1</sup> DA <sup>1</sup> ADSL <sup>1</sup> RY <sup>1</sup> Y <sup>358</sup>
IleRS	<sup>610</sup> T <sup>1</sup> VSPQDVM <sup>1</sup> NKL <sup>1</sup> GADI <sup>1</sup> LRL <sup>1</sup> W <sup>628</sup>

stable. In the case of the deletion from 177 to 499 ( $\Delta 177-499$ ), the diminished intensity of the resulting deletion protein is perhaps due to protein instability. There is a somewhat decreased intensity for the  $\Delta 328-444$  protein.

In extracts that contained the deletion proteins, the Ile-tRNA synthetase activity was checked by the aminoacylation assay and, in some cases, by the isoleucine-dependent ATP-pyrophosphate exchange assay. Aminoacylation requires both amino acid activation and transfer of the activated amino acid to tRNA. The exchange assay monitors only the activation step. These assays were done with deletion plasmid constructs in a *recA*<sup>-</sup> version of strain M11 which harbors a mutant Ile-tRNA synthetase that has a 300-fold higher Michaelis constant ( $K_m$ ) for isoleucine than that for the wild-type strain (25). Under the assay conditions, crude extracts of M11 have no isoleucine-dependent aminoacylation of tRNA (see below).

We compared the activities in extracts of M11 transformed with various deletion plasmids versus untransformed M11 and versus extracts of an untransformed control strain DH1 (Fig. 5) (26). Activities were normalized to a constant amount of extract protein. Extracts of cells with three of the deletion plasmid constructions had significant activi-

ty that was well above the amount contributed by the single wild-type *ileS* allele of DH1. The active extracts were from cells that harbor deletions  $\Delta 231-276$ ,  $\Delta 276-329$ , and  $\Delta 276-377$ . Each remaining deletion protein showed no activity because it was either intrinsically inactive or unstable (as is suggested for the  $\Delta 177-499$  protein in Fig. 4).

Since Ile-tRNA synthetase is a monomer (6), it is unlikely that the active deletion proteins function by associating with the inactive M11 protein. Moreover, if the deletion proteins were inactive and were able to associate with and activate the M11 protein, it is unlikely that activity in excess of that in extracts of DH1 could be generated.

For each of the three active deletion proteins, we also constructed frameshift variants of the relevant plasmid. The introduction of a frameshift at codon 177 creates a TGA stop 44 codons later. These constructions failed to produce full length protein and were inactive in the M11 strain background. This argues against the possibility that activity is generated by the active deletions through a marker rescue mechanism in which genetic recombination yields a wild-type Ile-tRNA synthetase. Further evidence against this possibility is the detection of amplified protein of the expected size in extracts of strains harboring the deletion

plasmids (Fig. 4). Therefore, we surmise that the deletions lacking residues between codons 231 and 377 encode proteins that are intrinsically active. They probably have  $K_m$  values for isoleucine that are not much higher than that of the wild-type enzyme because activity is easily detected at 20  $\mu M$  isoleucine.

In cases where aminoacylation activity was detected, we confirmed the presence of enhanced isoleucine-dependent ATP-pyrophosphate activity (Fig. 3). The four internal deletions that lack aminoacylation activity also lack the exchange activity.

We used a modified Chou-Fasman algorithm (27, 28) to determine that  $\alpha$  helices and  $\beta$  strands have the potential to form in Ile-tRNA synthetase in regions comparable to those of the nucleotide fold in Met-tRNA synthetase (Fig. 6). According to the alignment and structure in Figs. 1, 2, and 6, removal of amino acids 232 to 376 would correspond to a large deletion from the middle of the segment designated CP1, a part that is well removed from any of the prototypical secondary structure elements. The other deletions remove sequences on either side of amino acids 232 or 376, and come close to or actually extend into known elements of secondary structure in the methionine enzyme.

Some structural similarity between the methionine enzyme and the tyrosine enzyme from *B. stearohermophilus* has been noted (18). Tyrosyl-tRNA synthetase is a dimer of 419 amino acid subunits that are less than half the size of Ile-tRNA synthetase (6, 29). This size difference is reflected in the nucle-

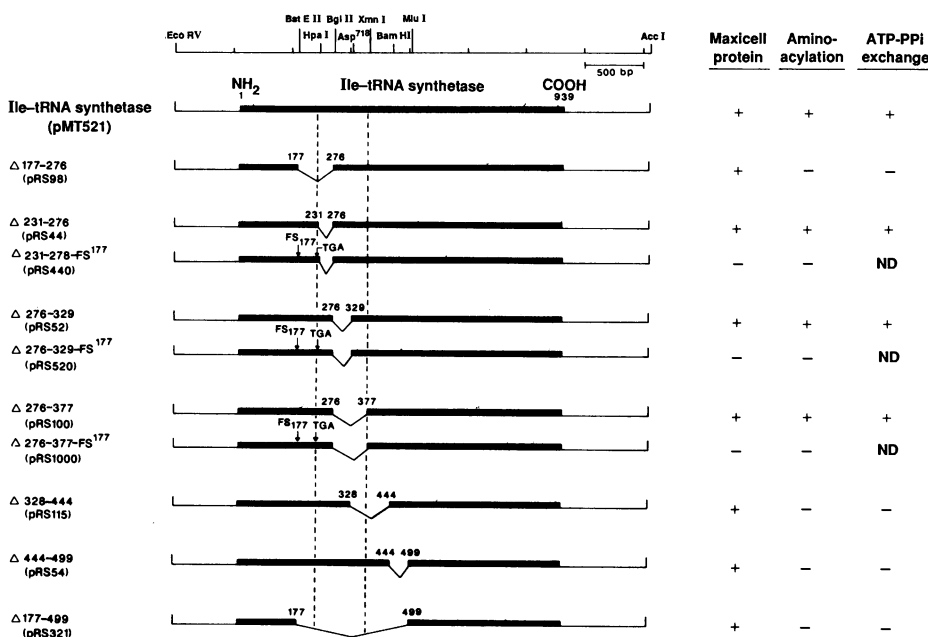


**Fig. 3.** Internal deletions of Ile-tRNA synthetase. The top line shows the *ileS*-containing insert of pMT521 with the restriction sites used for deletion constructions (37). The coding region is indicated by the heavy line and amino acids joined together in each deletion are noted. Insertion of an extra amino acid at the junction has no apparent effect on activity. FS177 indicates the site of a frameshift produced by filling in the Bst EII site which results in the indicated TGA stop. The dotted lines bracket the region defined as dispensable for activity by the active deletions (ND, not determined). All deletions were made by digestion of the parent plasmid pMT521 (37) and other related plasmids with the appropriate enzymes and filling in of sticky ends where needed. Ligations were in the presence of low melting point agarose, and constructions were analyzed for loss of key restriction sites and the appearance of short characteristic fragments (38). See legends to Figs. 4 and 5 for maxicell and enzyme assay methods.

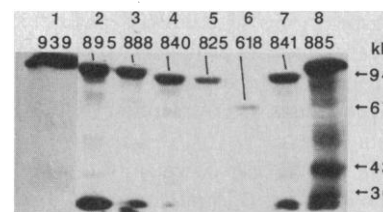


**Fig. 4.** Maxicell analysis of internal deletions of Ile-tRNA synthetase. Lane 1, wild-type (pMT521); lane 2,  $\Delta 231-276$  (pRS44); lane 3,  $\Delta 276-329$  (pRS52); lane 4,  $\Delta 276-377$  (pRS100); lane 5,  $\Delta 328-444$  (pRS115); lane 6,  $\Delta 177-499$  (pRS321); lane 7,  $\Delta 444-499$  (pRS54). Polypeptide sizes of the wild-type enzyme and the seven deletions are indicated above their respective lanes and are as predicted from the gene sequences. Size markers (Pharmacia) are indicated on the right. The  $\beta$ -lactamase polypeptide (about 30,000 daltons) is visible in some lanes. The plasmid encoded wild-type and deletion proteins were visualized with the use of the maxicell technique (24) in strain DH1 (26). The [<sup>35</sup>S]methionine (1250 Ci/mmol, Amersham)-labeled proteins were separated on a Laemmli gel (39) (3% stacking, 10% running), soaked in Autofluor (National Diagnostics), dried onto filter paper, and exposed to x-ray film.

tide fold which, at about 220 amino acids (11, 12), is considerably smaller than the 628 residues of the putative domain of isoleucyl-tRNA synthetase. A diagrammatic representation of the tyrosine enzyme like that of Fig. 6 suggests there may be little in the way of dispensable peptide sequences in Tyr-tRNA synthetase.

This analysis of isoleucyl-tRNA synthetase supports the hypothesis that variations in synthetase subunit sizes arise from the addition of residues (dispensable for cataly-

sis) to an active core structure (6). This is the first identification of expendable internal sequences. Earlier reports describe dispensable COOH-terminal fragments in alanyl- and methionyl-tRNA synthetases (1, 13, 14).

Because large deletions in the putative CP1 part of Ile-tRNA synthetase do not destroy activity, we reason that a portion of CP1 must lie on the surface of the protein where its removal does not disturb the internal structure. It is known that CP1 is on the

surface of Met-tRNA synthetase (8-10). Our results, in conjunction with the known structure of Met- and Tyr-tRNA synthetases, suggest that nucleotide folds might be able to accommodate insertions into the core domain. Inspection of four well-characterized dehydrogenase structures shows that their nucleotide binding domains contain relatively few residues extraneous to the prototypical Rossmann fold (7). Whether insertions between  $\beta_C$  and  $B_D$  can be accommodated in these enzymes is unknown. Such insertions might, in turn, be engineered to create chimeric nucleotide binding enzymes. For example, CP1 could be a prime spot for connections to make chimeric synthetases for structure-function determinations.

**Fig. 5** Aminoacylation activity of Ile-tRNA synthetase constructs. Symbols associated with each experimental point are defined within the figure. Assays were performed in triplicate at 37°C. For the active deletion proteins, all experimental points are within 16% of the reported average. Fluctuations of the 8-minute point around the mean are similar to that for the other points and the apparent dip in activity is within experimental error. The constructs with no activity are similar to that of MII alone whose results are shown here. Activities were normalized to a constant amount of protein (Bio-Rad). A *recA* variant of *E. coli* strain MII (25) was transformed with the various deletion plasmids. This strain harbors a mutant Ile-tRNA synthetase with a  $K_m$  for isoleucine that is 300-fold above that of the wild-type enzyme. Cell extracts (40) were assayed at 20  $\mu M$  isoleucine (aminoacylation) or 100  $\mu M$  isoleucine (ATP-pyrophosphate exchange) (38). The presence of all seven deletion proteins in the extracts was confirmed by immune-blot analysis (41) with polyclonal antibodies against denatured wild-type Ile-tRNA synthetase.

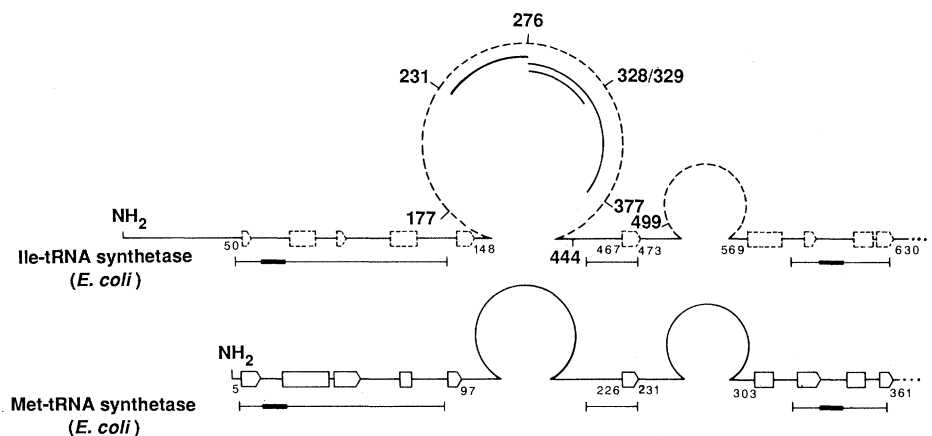
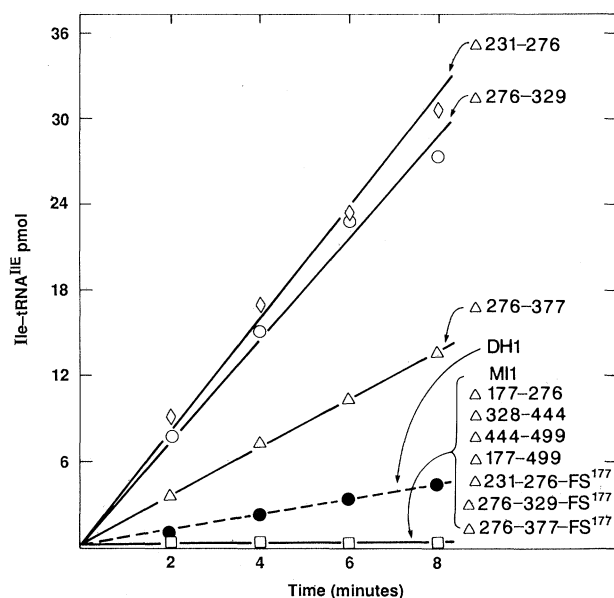


**Fig. 6** Structural comparison of Met- and Ile-tRNA synthetases. Secondary structure elements of the prototypical Rossmann fold of Met-tRNA synthetase are indicated as rectangles ( $\alpha$  helices) or pentagons ( $\beta$  strands) along the primary sequence with boundaries given in small numbers. Regions of amino acid sequence similarity between the two enzymes are underlined, and dark bars indicate the signature sequence and the alignment of the cross-link site for the 3' end of tRNA on Met-tRNA synthetase with a sequence in Ile-tRNA synthetase. CP1 and CP2 are bulges above the line. In Ile-tRNA synthetase deletion boundaries are indicated by the large numbers, and the extent of the three active deletions are shown as solid lines. Dotted rectangles and pentagons for Ile-tRNA synthetase indicate secondary structure predictions that are guided by the sequence similarities of Fig. 2; we have included a predicted  $\beta_C$  and  $\alpha_E$  in the region of no sequence similarity. Secondary structure predictions were carried out with a modified Chou and Fasman algorithm implemented by PRSTRC (28, 36).

#### REFERENCES AND NOTES

1. M. Jasin, L. Regan, P. Schimmel, *Nature (London)* **306**, 441 (1983).
2. ———, *Cell* **36**, 1089 (1984).
3. L. Regan et al., *Science* **235**, 1651 (1987).
4. F. V. Fuller-Pace et al., *Proc. Natl. Acad. Sci. U.S.A.* **81**, 6095 (1984).
5. V. Nagaraja, J. C. W. Shephard, T. A. Bickle, *Nature (London)* **316**, 371 (1985).
6. P. Schimmel, *Annu. Rev. Biochem.* **56**, 125 (1987).
7. M. G. Rossmann, A. Liljas, C.-I. Branden, L. J. Banaszak, in *The Enzymes*, P. D. Boyer, Ed. (Academic Press, New York, 1975), vol. 11A, p. 61.
8. J.-L. Risler, C. Zelwer, S. Brunie, *Nature (London)* **292**, 384 (1981).
9. C. Zelwer, J.-L. Risler, S. Brunie, *J. Mol. Biol.* **155**, 63 (1982).
10. S. Brunie, P. Mellot, C. Zelwer, J.-L. Risler, S. Blanquet, G. Fayat, *J. Mol. Graphics*, in press.
11. T. H. Bhat, D. M. Blow, P. Brick, J. Nyborg, *J. Mol. Biol.* **158**, 699 (1982).
12. D. M. Blow and P. Brick, in *Biological Macromolecules and Assemblies: Nucleic Acids and Interactive Proteins*, F. Jurnak and A. McPherson, Eds. (Wiley, New York, 1985), vol. 2, p. 442.
13. D. Cassio and J. P. Waller, *Eur. J. Biochem.* **20**, 283 (1971).
14. D. Kohda, S. Yokoyama, T. Miyazawa, *J. Biol. Chem.* **262**, 558 (1987).
15. D. G. Barker, J.-P. Ebel, R. Jakes, C. J. Bruton, *ibid.* **127**, 449 (1982).
16. F. Dardel, G. Fayat, S. Blanquet, *J. Bacteriol.* **160**, 1115 (1984).
17. T. Webster, H. Tsai, M. Kula, G. A. Mackie, P. Schimmel, *Science* **226**, 1315 (1984).
18. D. M. Blow, T. N. Bhat, A. Metcalfe, J.-L. Risler, S. Brunie, C. Zelwer, *J. Mol. Biol.* **171**, 571 (1983).
19. Abbreviations for the amino acid residues are: A, Ala; C, Cys; D, Asp; E, Glu; F, Phe; G, Gly; H, His; I, Ile; K, Lys; L, Leu; M, Met; N, Asn; P, Pro; Q, Gln; R, Arg; S, Ser; T, Thr; V, Val; W, Trp; and Y, Tyr.
20. J. E. Walker, M. Saraste, M. J. Runswick, N. J. Gay, *EMBO J.* **1**, 945 (1982).
21. C. Hountondji, S. Blanquet, F. Lederer, *Biochemistry* **24**, 1175 (1985).
22. C. Hountondji, F. Lederer, P. Dessen, S. Blanquet, *ibid.* **25**, 16 (1986).
23. C. Hountondji, P. Dessen, S. Blanquet, *Biochimie* **68**, 1071 (1986).
24. A. Sancar, A. H. Hack, W. D. Rupp, *J. Bacteriol.* **137**, 692 (1979).
25. M. Iaccarino and P. Berg, *J. Bacteriol.* **105**, 527 (1971).
26. B. Low, *Proc. Natl. Acad. Sci. U.S.A.* **60**, 160 (1968).
27. P. Y. Chou and G. D. Fasman, *Annu. Rev. Biochem.* **47**, 251 (1978).
28. W. W. Ralph, T. A. Webster, T. F. Smith, *CABIOS*, in press.
29. G. Winter, G. L. E. Koch, B. S. Hartley, D. G. Barker, *Eur. J. Biochem.* **132**, 383 (1983).

30. M. S. Waterman, *Bull. Math. Biol.* **46**, 473 (1984).  
 31. T. F. Smith and M. S. Waterman, *J. Mol. Biol.* **147**, 195 (1981).  
 32. R. Doolittle, *Science* **214**, 149 (1981).  
 33. T. J. Borgford, N. J. Brand, T. E. Gray, A. R. Fersht, *Biochemistry* **26**, 2480 (1987).  
 34. X. Jordana, B. Chatton, M. Paz-Weishaar, J.-M. Buhler, F. Cramer, J.-P. Ebel, F. Fasiolo, *J. Biol. Chem.* **262**, 7189 (1987).  
 35. P. Rainey, E. Holler, M.-R. Kula, *Eur. J. Biochem.* **63**, 419 (1976).  
 36. Details are available upon request from T. Webster.  
 37. M. Tokunaga, J. M. Loranger, H. Wu, *J. Biol. Chem.* **258**, 12102 (1983).  
 38. Details are available upon request from R. Starzyk.  
 39. U. K. Laemmli, *Nature (London)* **227**, 680 (1970).  
 40. M. J. Toth and P. Schimmel, *J. Biol. Chem.* **261**, 6643 (1986).  
 41. H. Towbin, T. Staehelin, J. Gordon, *Proc. Natl. Acad. Sci. U.S.A.* **76**, 4350 (1979).  
 42. Supported by NIH grant No. GM23562. We thank D. Blow and S. Brunie for helpful comments on the manuscript; S. Brunie for providing us with structural information on *E. coli* Met-tRNA synthetase prior to publication; H. Wu for plasmid pMT521; Z. Altboum for polyclonal antibodies to Ile-tRNA synthetase; M. Härtlein for transmitting the sequence of *E. coli* Val-tRNA synthetase prior to publication; and B. Bachmann for *E. coli* strains M11 and DH1.

10 March 1987; accepted 22 June 1987

## Direct Demonstration of Macula Densa-Mediated Renin Secretion

OLE SKØTT AND JOSEPHINE P. BRIGGS\*

An *in vitro* method has been used to examine whether secretion of renin from the juxtaglomerular apparatus is affected by changes in the sodium chloride concentration of the tubular fluid at the macula densa. Single juxtaglomerular apparatuses were microdissected from rabbits and the tubule segment containing the macula densa was perfused, while simultaneously the entire juxtaglomerular apparatus was superfused, and the fluid was collected for renin measurement. In this preparation, in which influences from renal nerves and local hemodynamic effects are eliminated, a decrease in the tubular sodium chloride concentration at the macula densa results in a prompt stimulation of the renin release rate.

**R**ENIN IS AN ASPARTYL PEPTIDASE that is synthesized, stored, and released from granular cells in the renal vasculature (1). It catalyzes the cleavage of the decapeptide angiotensin I (AI) from angiotensinogen; AI is in turn transformed by converting enzyme to the physiologically active form, angiotensin II (AII). The active form AII is both a potent vasoconstrictor, with a regulatory role in control of renal and systemic vascular resistance, and a regulator of salt balance by promoting aldosterone release. Increased activity of the renin-angiotensin system may cause certain forms of hypertension. In keeping with its complex homeostatic roles, the regulation of renin secretion is under control of a number of factors. Release is stimulated by decreases in arterial pressure and increases in activity of the renal nerves (2); it is also probably influenced by the local concentrations of a variety of substances including prostaglandins, catecholamines, AII, and adenosine (2).

The renin-containing granular cells are located primarily at the glomerular vascular

pole in the juxtaglomerular apparatus (JGA). This cell complex consists of three cell types—the granular cells, which contain renin, modified interstitial cells, and a specialized plaque of tubular epithelial cells called the macula densa. The macula densa is located in the wall of the thick ascending limb of Henle at the point where the tubule returns to its parent glomerulus. Sodium chloride concentration in tubular fluid at the macula densa varies widely with the physiological state of the animal and the flow rate in the tubule. In salt-depleted states, where tubular flow rate is slowed, NaCl concentration falls to low values (20 to 40 mM); it rises toward isotonic values in volume-expanded states where tubular flow rate is increased (3–5). This unique structural arrangement led, in 1944, to the proposition that renin release might be under control of tubular function at this site in the nephron (6).

It has, however, proven difficult to establish whether tubular fluid composition at the macula densa in fact influences renin release. The evidence usually cited to support macula densa-mediated renin release is indirect and inferential (7). Even the direction of change in renin secretion rate after changes in the tubular fluid composition is controversial. Two contradictory theories have emerged: one group of investigators

propose that an increase in NaCl concentration at the macula densa (8–11) is a local signal for renin secretion, whereas others have maintained that renin release responds to a fall in NaCl concentration (4, 12–15).

A number of methods have been used to attempt to resolve this issue. Experimental preparations such as the “nonfiltering kid-



**Fig. 1.** Single JGA microperfusion. An individual JGA, consisting of portions of the thick ascending limb of Henle, macula densa, and early distal tubule with adherent glomerulus and hilar structures, was dissected from New Zealand white rabbits (body weight, 1.0 to 1.75 kg) and transferred to a thermoregulated chamber mounted on an inverted microscope. (A) The tubule was cannulated and perfused with a modified isolated perfused tubule apparatus (24, 25). The distal end was not cannulated. The tubular perfusion rate was maintained by a hydrostatic pressure gradient at about 10 nl per minute. Scale bar, 100  $\mu$ m. (B) After perfusion had been established the macula densa could be visualized (arrows). Scale bar, 25  $\mu$ m. An outer pipette was advanced to cover the perfused JGA. Flow was maintained at a rate of 600 nl/min through the outer superfusion pipette. After an equilibration period of 15 minutes, fluid in the bath chamber was replaced with warmed mineral oil. The droplets of superfusate that formed at the tip of the outer pipette were collected at 10-minute intervals for renin assay. Renin released from the JGAs was measured by radioimmunoassay of generated AI with the antibody-trapping technique (20). The sample was added to 20  $\mu$ l of a mixture of purified AI antibody and purified renin substrate (1200 ng of AI per milliliter) and incubated for 24 hours at 37°C with subsequent radioimmunoassay of generated AI. After the experiments, the renin was extracted from the JGAs by freezing and thawing four times. Renin is expressed in terms of Goldblatt units compared to standards from the Institute for Medical Research (M.R.C., Mill Hill, London). The detection limit of the assay was found to be 1 nGU contained in 5  $\mu$ l, which is equivalent to 160 fg of AI generated per hour of incubation.

Department of Internal Medicine, University of Michigan, Ann Arbor, MI 48109.

\*To whom correspondence should be addressed at Division of Nephrology, University of Michigan Medical Center, 3914 Taubman Center, Ann Arbor, MI 48109.